Korean J. Chem. Eng., 35(3), 662-670 (2018)
DOI: 10.1007/s11814-017-0325-5

pISSN: 0256-1115
eISSN: 1975-7220

Fabrication of polypyrrole composite on perlite zeolite surface and its application for removal of copper from wood and paper factories wastewater

Ali Naghizadeh[*,,†], Seyyed Jalal Mousavi[***], Elham Derakhshani[**], Mohammad Kamranifar[**], and Seyyed Meysam Sharifi[***]**

*Medical Toxicology and Drug Abuse Research Center (MTDRC), Birjand University of Medical Sciences (BUMS), Birjand, Iran
**Department of Environmental Health Engineering, Faculty of Health, Birjand University of Medical Sciences, Birjand, Iran
***Department of Engineering, College of Natural Resources, Islamic Azad University, Bandar Abbas Branch, Bandar Abbas, Iran
(*Received 31 March 2017 • accepted 22 November 2017*)

Abstract−The large volumes of water used in wood and paper industries produce substantial amounts of wastewater. These industries are among the most polluting ones in the world; there are large quantities of heavy metals (copper, iron, zinc, etc.) and dyes in the wastewater of these industries, and this wastewater has high levels of COD and BOD. We studied copper removal from the effluents of a wood and paper factory by using a polypyrrole composite consisting of natural Zeolite coated on Perlite (PPy/Perlite). The experiments were performed in a batch system in which effects of various parameters including pH, contact time, adsorbent dosage, and temperature on adsorption were studied. Moreover, SEM and FTIR were employed to identify the structure of the synthesized adsorbent. Results indicated that the maximum copper removal (95%) happened at pH=6, contact time of 12 minutes, and adsorbent dose of 0.4 g/100 mL of the wastewater. Furthermore, copper adsorption capacity of the PPy/Perlite adsorbent improved with increases in temperature and reached its peak at 40 °C. Values of the thermodynamic variables (ΔS, ΔH, ΔG) indicated that copper adsorption could occur in the temperature range of 293-323 Kelvin, and was spontaneous and endothermic. Equilibrium information in the studied range of the initial concentrations of copper and in the temperature range suitably matched the Freundlich isotherm. Evaluation of experimental information for studying the kinetics of copper adsorption by PPy/Perlite revealed that copper adsorption followed the pseudo-second-order kinetic model.

Keywords: Polypyrrole, Natural Zeolite, Perlite, Wood and Paper Factory, Copper

INTRODUCTION

The rapid increase in population and the growing demand of industrial facilities for resources in order to satisfy human needs have caused problems such as overexploitation of available resources and soil, air, and water pollution. Wood and paper industries, which are the fifth most important among the industries in developed countries including the USA, are no exception to this general rule and produce substantial quantities of pollutants, including heavy metals (copper, iron, zinc, etc.), high levels of COD and BOD, and considerable amounts of dyes that enter the receiving waters either untreated or slightly treated. The large volumes of water used in the production of each ton of products lead to the production of great amounts of wastewater, and place the wood and paper industries among the most polluting industries in the world. Presence of copper in the human body beyond the permissible limits leads to complications such as headache, reduced blood sugar, high heart rates, and nausea. The excess copper precipitates in the brain and liver, damages the kidneys, and causes anemia. Copper poisoning in children is related to hyperactivity, learning disorders such as reading and writing disorders, attention deficit disorder, and ear infections [1,2].

Therefore, the removal of copper from polluted aquatic systems has attracted increasing attention. Several technologies, including chemical precipitation, reverse osmosis, ion-exchange, electrochemical process and adsorption have been developed [3-5]. Among these, adsorption is widely used in treating wastewater and gas in the chemical industry [6,7]. Adsorption is a simple, highly efficient and easy operation [8]. Also the adsorbent can be reused in long-term applied programs [6,9]. Adsorbents may be organic or inorganic. Inorganic adsorbents are superior to organic ones with respect to mechanical strength and chemical stability, specific surface, and stability against microbial decomposition. Compounds such as activated carbon, natural Zeolites, bentonite, chitosan, corncob wood, rice husk, barley bran, and dry activated sludge have been used as adsorbents [10,11]. Activated carbon is the most common adsorbent, and is used in removing various pollutants [12]. But activated carbon is expensive. Therefore, searching for low cost adsorbents is important [13].

So far, numerous studies have been conducted to remove pollution caused by copper. Bhattacharyya et al. studied removal of copper ions from aqueous solutions by several types of natural clay soil and clay soil activated by acid. According to the Langmuir isotherm model, the maximum single layer adsorption capacity of an adsorbent is in the 9.2-32.3 mg/g range [14]. Ji et al. prepared fibers of cellulose acetate/Zeolite composite and used them to remove

†To whom correspondence should be addressed.
E-mail: al.naghizadeh@yahoo.com, aliinaghizadeh@gmail.com

copper and nickel ions from an aqueous solution. They noticed that adsorption efficiency of metal ions was higher at high pH values compared to acidic environments. Kinetic data could be well predicted using the pseudo-second-order kinetic model, and equilibrium time for the adsorption reaction of copper and nickel ions on CA/Z was 36 hours. Equilibrium data also matched the Langmuir model. The maximum adsorption capacity for Cu(II) on CA/Z was 28.57 mg/g at room temperature [15].

Polypyrrole (PPy) and most of its derivatives can be synthesized using simple chemical and/or electrochemical methods. Large volumes of polypyrrole can be produced as a powder by polymerizing monomer oxide and/or through employing chemical oxidants [16-18]. Our aim was to study copper adsorption from effluents of a wood and paper factory using a polypyrrole composite adsorbent that was based on natural Zeolite and Perlite. The experiments were performed in a discontinuous system and the effects of parameters such as pH, contact time, adsorbent dose, and temperature on copper adsorption from effluents of the wood and paper factory were studied. Finally, Langmuir, Freundlich, Temkin, and Dubinin-Radushkevich isotherms, the Morris-Weber model of adsorption kinetics, and the pseudo-first-order and second-order kinetic models were employed to investigate the adsorption process. Moreover, the thermodynamics of the process of copper adsorption from effluents of the wood and paper factory by the polymeric composite was investigated.

MATERIALS AND METHODS

1. Materials

Effluents of the Wood and Paper Factory of Mazandaran with characteristics listed in Table 1 were used in the study, and 1 N hydrochloric acid (HCl) and sodium hydroxide (NaOH) to adjust the pH, and a pyrrole monomer, $FeCl_3$, and Perlite to synthesize the composite. Perlite was obtained from the Afrazand Company and the rest of the materials were bought from the Merck Company.

Table 1. Characteristics of the effluents from the wood and paper factory of mazandaran

Compound	Concentration in waste water before removal
Cu (mg/L)	4.5
Mg (mg/L)	300
Fe (mg/L)	1.5
Zn (mg/L)	16
Total N(NO_3^{-1}, NO_2^{-1}) (mg/L)	33
S^{-2} (mg/L)	21
SO_4^{-2} (mg/L)	155
Color (adsorbance at 600 nm)	0.3612
COD (mg/L)	2700

2. Characteristics of the Adsorbent

SEM images were employed to determine the surface area of the adsorbent. Before taking the images, the surface was covered with a 30 nm-thick coating of gold using a sputter coater to improve the conductivity of the materials and obtain high quality images. An FTIR instrument was used to identify functional groups. One mg of the adsorbent was mixed with 1,000 mg of KBr to form a uniform mixture, and the mixture was pressed on a transparent disk for five minutes under the pressure of 200 kgf/cm^2. The prepared sample was then ready for the FTIR test. The scan range for the samples was 600-4,200 cm^{-1}.

3. Perlite Preparation

Perlite was first washed several times with double distilled water, dried in an oven at 110 °C for 24 hours, and the granules were then ground and passed through a 200 mesh screen. The perlite was then put in a furnace at 550 °C for 5 hours to eliminate all impurities. 5 grams of the perlite were poured into 100 mL of 0.06 N sulfuric acid and stirred at 87 °C for 2 hours to be activated, washed several times with double distilled water, and dried in an oven at 110 °C for 24 hours [19]. The chemical composition of the perlite, which was determined using XRF analysis and is shown in Table 2, matched that presented in the references [20].

4. Synthesis of PPy/Perlite

5 grams of $FeCl_3$ were added to 100 mL of water and stirred until a completely uniform solution was obtained. 1 gram of perlite was then added to the solution followed by 1 mL of pyrrole monomer and the mixer was put on a mixer for 4 hours at room temperature. Filter paper was then used to separate the precipitate from the solution, was washed several times using distilled water, and then dried at room temperature. This synthetic process yielded about 1-2 g of the black colored adsorbent [21,22].

5. Adsorption Experiments

These experiments were performed using a stirrer in a discontinuous system. After the initial filtration of the wastewater for removing suspended solid particles, the samples were ready for the adsorption process. Each solution had a volume of 100 mL, the adsorbent was separated from the solution after each experiment through filtration, and the sample was prepared for analysis. An atomic adsorption spectrophotometer with a graphite furnace atomizer was employed to measure the quantity of copper in the wastewater.

5-1. Optimum pH

In this stage, the necessary preparations were made, the pH values of the samples were adjusted between 2 and 6, and the experiments were conducted with the contact time of 12 minutes at 20 °C using a stirrer at 400 rpm.

5-2. Optimum Contact Time

As in the previous stage, the wastewater was prepared and samples with the optimum pH and adsorbent dose of 0.4 g/100 mL were used to perform the adsorption experiment at various con-

Table 2. Chemical composition of the perlite determined by XRF

Materials	L.O.I	S	P_2O_5	MnO	TiO_2	Na_2O	MoO_3	K_2O	MgO	CaO	Fe_2O_3	Al_2O_3	SiO_2
Wt%	0.89	0.015	0.008	0.072	0.069	3.52	3.835	5.21	0.02	0.78	0.85	11.74	72.68

tact times (2-16 minutes).

5-3. Optimum Adsorbent Dosage

Various doses of the adsorbent (0.05-0.5 g/100 mL of the wastewater) were then used for removing copper from the wastewater by PPy/Perlite under the conditions of optimum pH and contact time.

5-4. Effects of Temperature on Adsorption

In this stage, the effects of temperatures in the 20-40 °C range on copper removal efficiency were studied under the conditions of optimum pH, contact time, and adsorbent dose determined in the previous stages. Finally, Eq. (1) was employed to determine copper removal efficiency:

$$\% \text{ Removal} = \frac{(C_i - C_f)}{C_i} \times 100 \quad (1)$$

where C_i is the initial and C_f the final concentrations of the adsorbed materials [23].

6. Adsorption Isotherms

Langmuir's theory explains single-layer coating of the adsorbed material on a homogeneous adsorptive surface. This isotherm is based on the hypothesis that adsorption happens only once at each site and when it does no more adsorption can take place on the site. Langmuir's equation is presented below:

$$q_e = \frac{q_0 K_L C_e}{(1 + K_L C_e)} \quad (2)$$

where q_e is the equilibrium adsorption capacity, C_e the equilibrium concentration, and q_0 the maximum amount of single-layer adsorption (q_0 can also be called the theoretical adsorption capacity).

This equation must be linearized to obtain the equation constants K_c and q_0. Eq. (3) presents the linearized form of this isotherm:

$$\frac{C_e}{q_e} = \frac{1}{q_0 \cdot K_L} + \frac{1}{q_0} C_e \quad (3)$$

A line is obtained by plotting C_e/q_e against C_e. The slope of this line and its y-intercept can be used to obtain q_0 and K_L, respectively [24,25].

Contrary to the Langmuir equation, the Freundlich equation is based on a heterogeneous surface. In the Langmuir equation, it is assumed that adsorption enthalpy is independent of the amount of adsorption, but the assumption in thte Freundlich isotherm is that adsorption enthalpy experiences a logarithmic decrease with increases in the number of occupied adsorption sites. The Freundlich isotherm equation is as follows:

$$q_e = K_F (C_e)^{1/n} \quad (4)$$

where K_F and 1/n are Freundlich constant and adsorption intensity, respectively. The equation must be linearized first to obtain these constants:

$$\text{Log}(q_e) = \log(K_F) + \frac{1}{n} \log(C_e) \quad (5)$$

The values for n and K_F can be obtained by calculating the slope and the y-intercept of the line derived from the above equation [24,25].

The Dubinin-Radushkevich model was used to analyze the data:

$$\ln(q_e) = \ln(q_m) - \beta\varepsilon^2 \quad (6)$$

where q_e is the equilibrium adsorption capacity, q_m the maximum adsorption, β the equation constant, and ε the Polanyi potential expressed in Eq. (7):

$$\varepsilon = RT \ln\left[1 + \left(\frac{1}{C_e}\right)\right] \quad (7)$$

where R is the universal gas constant, T temperature in Kelvin, and C_e the equilibrium concentration. By plotting ln q_e against ε^2, we obtain a line, and can use the slope and the y-intercept of this line to derive the values of q_m and β, respectively [26].

7. Kinetics of the Adsorption Process

The pseudo-first and second-order kinetic models and the Morris-Weber model of adsorption kinetics were used to study the adsorption process. The Morris-Weber equation is as follows:

$$q_t = K_{id}(t)^{0.5} + C \quad (8)$$

where q_t (mg/g) is the amount of adsorption at t (min), K_{id} (mg/(g·min)$^{1/2}$ is the constant of the intra particle diffusion rate constant, and C (mg/g) a constant that gives an idea of the boundary layer thickness. If the diagram of q_t (mg/g) plotted against $t^{0.5}$ is linear, we can claim that the process is controlled by resistance against internal infiltration. The values of the constants C and K_w are obtained from the slope and y-intercept of the linear diagram of q_t (mg/g) plotted against $t^{0.5}$ [27].

The pseudo-first-order equation is in the forms of Eqs. (9) and (10):

$$\frac{dq_t}{dt} = k_1(q_{eq} - q_t) \quad (9)$$

$$\log(q_e - q_t) = \log q_e - \frac{k_1 t}{2.303} \quad (10)$$

where t is time (min), q_t (mg/g) the amount of adsorption at time t, and k_1 (1/min) the constant of the first order equation [27].

The pseudo-second-order equation is based on the extent of equilibrium capacity at which the rate of occupation of adsorption sites is assumed to correspond to the number of vacant adsorption sites squared. The pseudo-second-order equation is presented in the form of Eqs. (11) and (12):

$$\frac{dq_t}{dt} = k_2(q_{eq} - q_t)^2 \quad (11)$$

$$\frac{t}{q_t} = \frac{1}{k_2 q_e^2} + \frac{t}{q_e} \quad (12)$$

where t is time (min) and k_2 is the constant of the second order equation (gmg^{-1}min^{-1}). If we plot t/q_t against t, we can derive the values of the k_2 and q_e. The pseudo-first and second-order equations are capable of adjusting the reaction rate, but the rate of a chemical reaction must be determined by performing experiments [28].

8. Effects of Temperature on the Thermodynamics of the Adsorption Process

In this stage, all the optimum parameters determined from the previous stages (pH, contact time, adsorbent dose) were kept con-

stant, and the experiments were conducted at 20, 30, and 40 °C. The thermodynamic constants for adsorption including Gibbs free energy (ΔG), entropy changes (ΔS), and enthalpy changes (ΔH) were determined. In this stage, Eqs. (13), (14), and (15) were used to derive the thermodynamic constants:

$$kd = \frac{q_e}{C_e} \tag{13}$$

$$\Delta G^o = -RT\ln kd \tag{14}$$

$$\ln kd = -\frac{\Delta H^o}{RT} + \frac{\Delta S^o}{R} \tag{15}$$

where R is the universal gas constant (8.314 J/mol·K), T is the absolute temperature (K), and k_e the thermodynamic equilibrium constant [29,30].

RESULTS AND DISCUSSION

1. Structure of the Adsorbent

Fig. 1 presents SEM images showing the morphology of the Perlite before and after being coated with PPy. The polymer coated on the surface of the Perlite can be clearly observed in these images. Part b in Fig. 1, which is presented at greater magnification, shows the coated polymer particles are completely spherical and nanosized. Fig. 1(d) presents SEM images taken of the PPy/Perlite adsorbent after it was used to treat the wastewater from the wood and paper factory. The light-colored particles in these images represent the adsorbed materials. Two points are worth mentioning about the polymer coating: the size of Perlite particles and the monomer concentration. If the Perlite particles are very small, the coating process will be reversed: the Perlite particles will be coated on the polymer; and, if the monomer concentration exceeds the required level, this process will be repeated again. Therefore, the size of Perlite particles and the monomer concentration must be taken into account in the coating process [21].

FTIR was employed to study the structure of PPy/Perlite (Fig. 2). The peaks in FTIR clearly showed that the coated material on Perlite was PPy. The peak at 1,641 cm^{-1} indicates the presence of C-C and C=C bonds. Furthermore, the peak at 1,429 cm^{-1} signifies the presence of C-N bonds. The C-H bond and the N-H bonds had their peaks at 1,292 cm^{-1} and 10,641 cm^{-1}, respectively. Moreover, the bonds at 781 and 632 cm^{-1} stand for external C-H bonds. All these indicate the presence of PPy in the composite [21].

2. Effects of pH on Removal Efficiency

Fig. 3 presents the effects of pH on the efficiency of copper removal by PPy/Perlite. As shown, the maximum removal efficiency

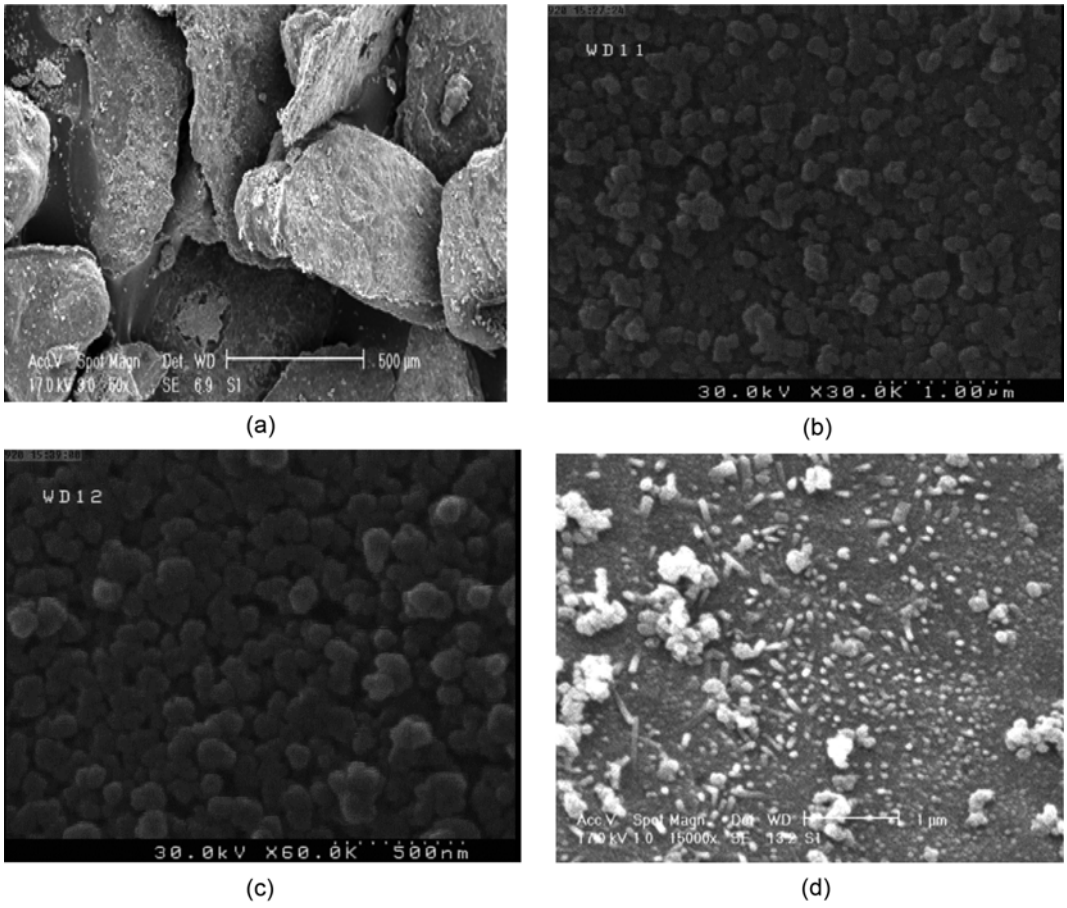

Fig. 1. SEM images of the adsorbent: (a) The Perlite before being coated with PPy, (b) the Perlite after being coated with PPy, (c) the Perlite after being coated with PPy (shown at greater magnification), (d) SEM images of PPy/Perlite after treatment of the wastewater from the wood and paper factory.

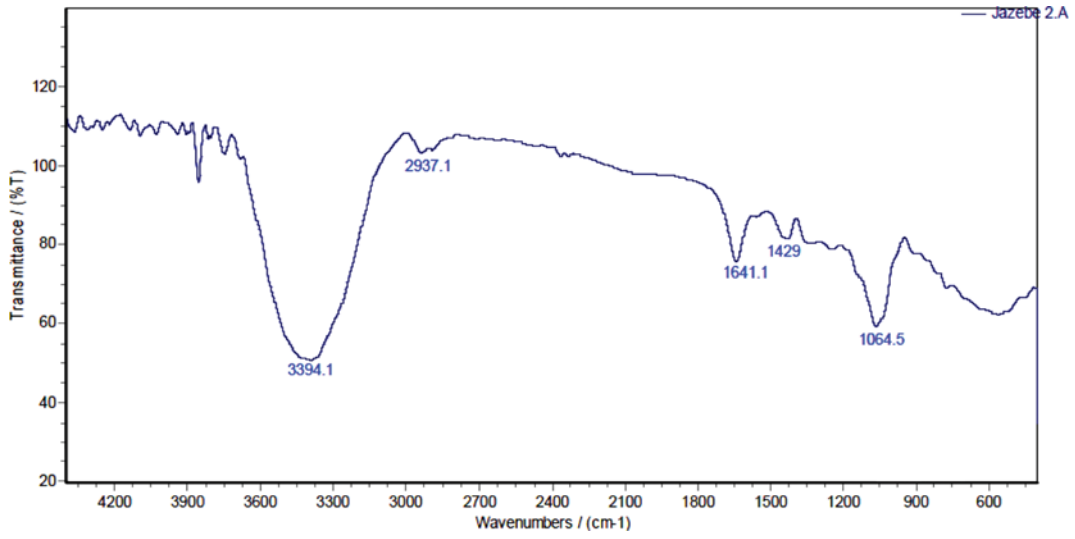

Fig. 2. The FTIR spectrum of the PPy/Perlite composite.

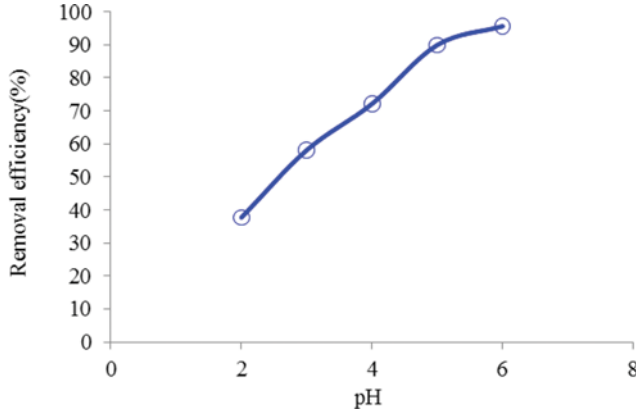

Fig. 3. The effect of pH on the removal efficiency of copper by PPy/Perlite.

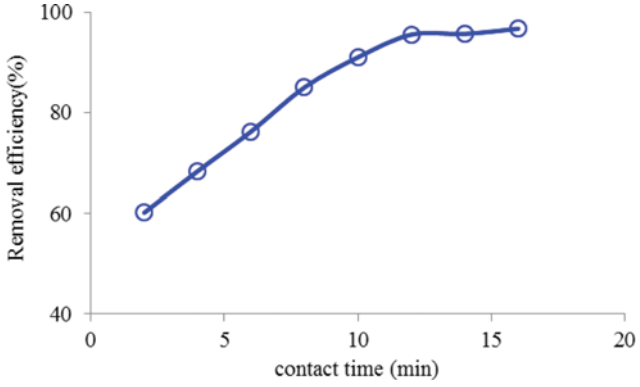

Fig. 4. The effect of contact time on the removal efficiency of copper by PPy/Perlite.

was achieved at pH=6. Previous research indicated that the pH of the solution was a factor influencing adsorption of heavy metals [6]. This parameter has an important effect on controlling the adsorbent surface charge, the degree of ionization of the solution, and the adsorption process [31]. At pH values higher than 6, copper is in the form of hydroxide ($Cu(OH)_2$), which precipitates in the solution. Therefore pH values higher than 6 were not tested for their effects on copper [3,32]. As seen in Fig. 3, removal efficiency increased with increases in pH values, and the maximum removal happened at pH=6. This could be attributed to the fact that at low pH values there is a competition between copper and H^+, which is caused by the presence of the hydrogen ions and which reduces copper adsorption [33]. Amarasinghe et al. obtained similar results in this relation [33].

3. The Effect of Contact Time on the Removal Efficiency

Fig. 4 shows the effect of reaction time on copper absorption by PPy/Perlite. pH=6 and absorbent dosage of 0.4 grams per 100 mL were determined as the experiment conditions. After 12 minutes the removal efficiency reached its maximum (%95.52) and after that there cannot be many changes in the removal efficiency. Therefore the reaction time of 12 minutes was selected as the optimal response time for the next series of experiments on copper absorption. This quick absorption could be due to excessive available surface at the start of the operation and it also indicates that absorption occurred mainly in the absorbent surface [34,35]. The results of this study corresponded to the work of Kuang et al. [36].

4. The Effect of Absorbent Dosage on the Removal Efficiency

Different dosages of absorbent (0.05-0.5 grams per 100 mL of effluent) were used to remove copper by PPy/Perlite under optimum conditions of pH and contact time. The results are shown in Fig. 5. Removal efficiency increases with the escalation of concentrations from 0.05 to 0.4 gram per 100 mL of effluent, but after this dosage, any increase in the absorbent does not have much impact on the removal efficiency. At a dosage of 0.4 grams per 100 cc the removal efficiency equals to %95.1. The mentioned increase in the absorption efficiency by raising the absorbent dosage can be thus explained that by increasing the absorbent, the number of active sites available for absorption of metal and anionic ions increases and as a result the absorption efficiency is increased, but after passing the optimal dosage of absorbent, the solution reaches equilibrium and then increasing the amount of absorbent will not have any signif-

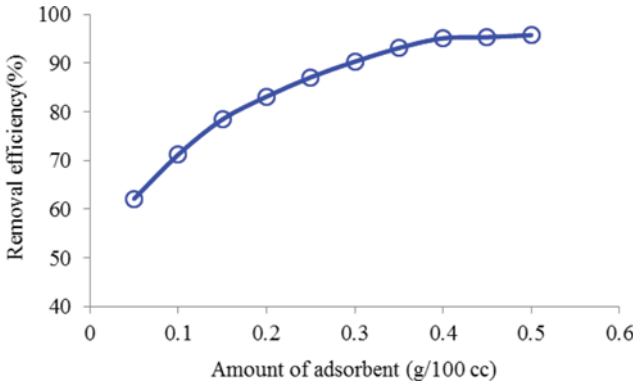

Fig. 5. Effect of absorbent dosage in the effluent on the removal efficiency of copper by PPy/Perlite.

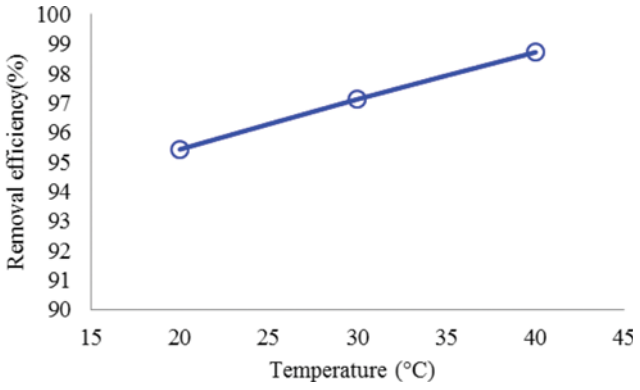

Fig. 6. The effect of temperature on the removal efficiency of copper by composite PPy/Perlite.

icant effect on absorption efficiency. This conclusion is similar to the findings of Chen et al. [37].

5. The Effect of Temperature on the Removal Efficiency and Thermodynamic Examination of the Process

The effect of temperature on the absorption efficiency in temperature range of 20 to 40 °C was examined. For copper absorption by absorbent composite, 6=pH, absorbent dosage of 4.0 grams per 100 mL of effluent and contact time of 12 minutes was determined. As one can see in Fig. 6, a rise in the temperature in this process also enhances the removal efficiency, although this increase is not significant. In this case, we can say that with increase in temperature, the process of absorption for copper (II), was actually a heat-absorbing reaction [8]. Similar results of copper absorption (II) in this manner were reported for modified bagasse cellulose [5].

Results of the study regarding the thermodynamic examination of the processes of copper absorption by PPy/Perlite are shown in Table 3. According to the results, the value of Gibbs free energy is

Table 3. Thermodynamic parameters copper absorption on PPy/Perlite

T °C	ΔG (KJ/mol)	ΔH (KJ/mol)	ΔS (KJ/mol.K)	R^2
20	−7.4			
30	−8.87	54.33	0.209	0.98
40	−11.31			

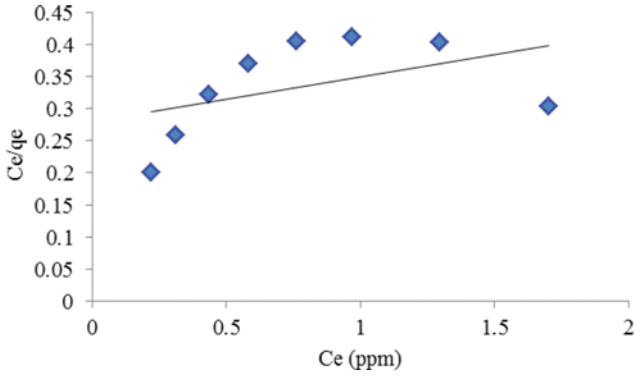

Fig. 7. Drawing linearized Langmuir equation for copper absorption on PPy/Perlite.

negative, which reflects that the nature of these processes is spontaneous. Further, ΔG can define the chemical or physical nature of the adsorption process. In this study, the values of ΔG are between 0 and −20 KJ/mol, which shows that the adsorption process is physical and is affected by van der Waals forces. Also, positive ΔH indicates that these two processes are endothermic. Positive ΔS reveals that the common level of solid and liquid phases increases accidentally when ions consolidate on the surface of adsorbents [38,39].

6. Examination of Absorption Isotherms

Langmuir isotherms, Freundlich and Dubinin-Radushkevich were calculated to analyze absorption isotherms. Langmuir isotherm model results are shown in Fig. 7. The correlation coefficient is low for copper absorption on PPy/Perlite, which shows that practically this equation is not suitable for the absorption process. The stats of this equation are shown in Table 4.

K_F and n Freundlich equation constants connects all factors affecting the absorption process such as absorption capacity and absorption rate. The constants of this equation are shown in Table 4. Fig. 8 shows a linearized model of the Freundlich equation for copper absorption on PPy/Perlite. An indication of an optimal absorption process in this equation is when the value of (n) is between 1 to 10.

Fig. 9 shows results obtained from the Dubinin-Radushkevich isotherm. As shown in this figure and in Table 4, the correlation coef-

Table 4. The isotherm equation and constants for copper adsorption on PPy/Perlite

Langmuir			Freundlich			Dubinin-Radushkevich		
q_m (mg/g)	K_L (L/mg)	R^2	K_F	n	R^2	q_m (mg/g)	β	R^2
3.57	4.0	0.22	2.7	1.4	0.91	2.72	0.000000006	0.70

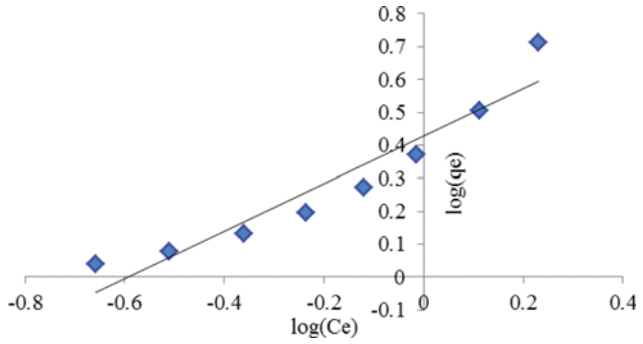

Fig. 8. The linearized Freundlich equation drawn for copper adsorption on PPy/Perlite.

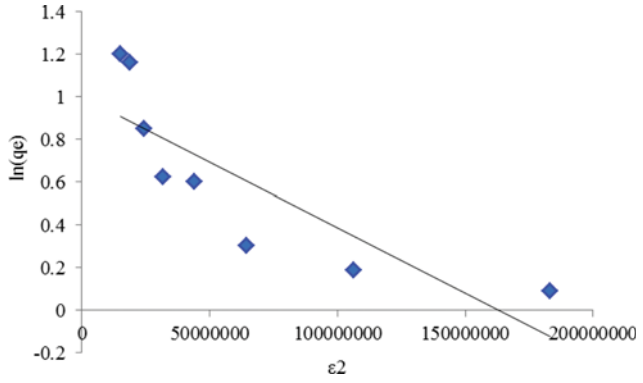

Fig. 9. The linearized D-R equation drawn for copper adsorption on PPy/Perlite.

ficient for copper adsorption on PPy/Perlite is very low, which indicates that this equation is not suitable for the adsorption process in this experiment.

Study of adsorption isotherms can lead to the description of how the reaction between the adsorbed material and the adsorbent takes place. As can be seen in Table 4, copper adsorption on PPy/Perlite with the R^2 of 0.91 followed the Freundlich isotherm to a very large extent, which indicated that the PPy/Perlite surface was not homogeneous and copper adsorption on it happened in several layers. Observations of other researchers conform to this result [40].

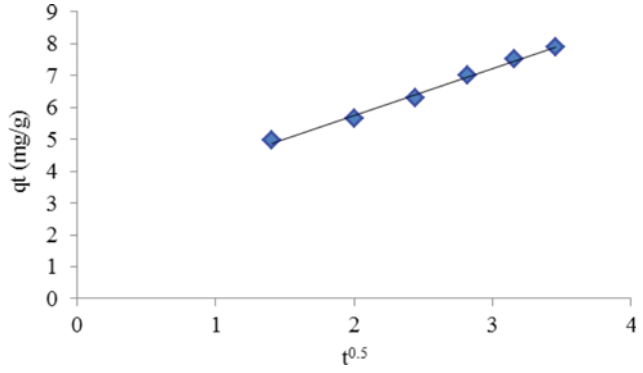

Fig. 10. The linearized Morris-Weber equation drawn for copper adsorption on PPy/Perlite.

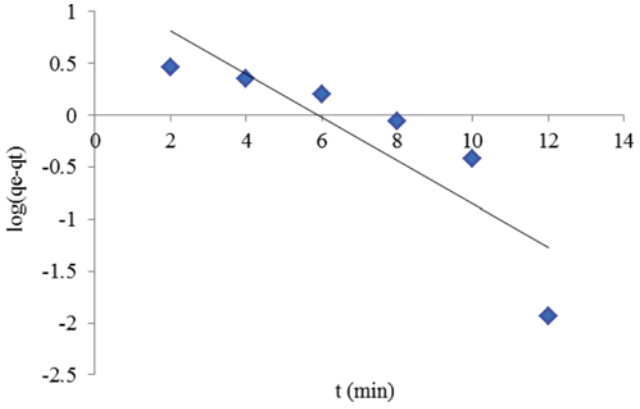

Fig. 11. The linearized pseudo-first-order equation drawn for copper adsorption on PPy/Perlite.

7. Kinetics of the Adsorption Process

In this section, the kinetics of the adsorption process was studied by using the Morris-Weber model and the pseudo-first and second-order kinetic models. In Fig. 10, q_t was plotted against $t^{0.5}$ in order to employ the Morris-Weber model. The constant of this equation (K_{id}) was obtained by calculating the slope of this line. K, the constant in the Morris-Weber equation for copper adsorption on PPy/Perlite, was 1.4753 min^{-1} and its correlation coefficient 0.9941.

Log (q_e−q_t) was plotted against t to carry out the calculations for the pseudo-first-order kinetic model (Fig. 11).The constant in this equation was the slope of the line, the constant for the pseudo-first-order kinetic equation for copper adsorption on PPy/Perlite was K_1=0.4795 min^{-1}, and the correlation coefficient for this diagram 0.7611.

Linearization of the pseudo-second-order equation was performed for making its calculations by plotting t/q_t against t. The slope of the line was then used to determine q_e, and the y-intercept of the line and the q_e value were then utilized to easily obtain the constant of this equation (Fig. 12). The constant of the pseudo-second-order equation and the correlation coefficient of the line for copper adsorption on PPy/Perlite were K_2=0.0487 min^{-1} and 0.9995, respectively.

Comparison of the data enabled us to easily notice that the results matched well with the pseudo-second-order equation, and we could

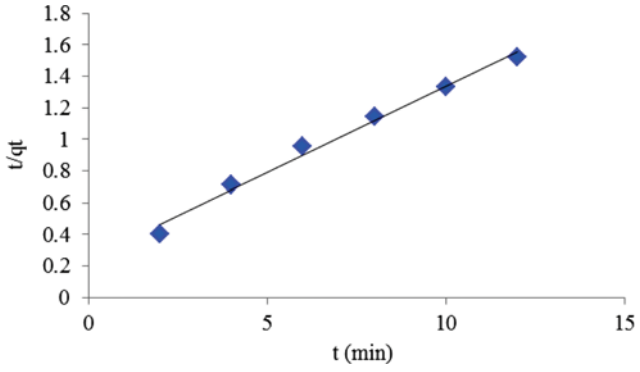

Fig. 12. The linearized equation of the pseudo-second-order equation drawn for copper adsorption on PPy/Perlite.

Table 5. Comparison of the maximum capacity (qm) of PPy/Perlite for copper with those of other adsorbents

Number	Adsorbent	Maximum adsorption capacity (mg/g)	Reference
1	PPy/Perlite	3.57	The present research
2	HA-SMZ	19.8	[42]
3	Chitosan/Zeolite composite (CZ)	25.88	[43]
4	Cellulose acetate/Zeolite (CA/Z)	28.57	[15]
5	B_2O_3/TiO_2 nanoparticles	82	[44]
6	Iron oxide on sand nanoparticles	1.26	[45]

say that the adsorption process was controlled by the pseudo-second-order equation. Of course, the Morris-Weber equation also matched well with these results. Before discussing this subject, we must refer to two points. First, the amount of adsorption is directly related to the presence of the materials and to their concentrations in the aqueous solution. Second, the second stage of the infiltration is largely based on high concentrations of the adsorbent. As previously mentioned, results matched the pseudo-second-order equation very well. The pseudo-second-order equation was the limiting stage in our process, and it required equilibrium between the attractive force and division of electrons and/or electron exchange between the adsorbent and the adsorbed material. Finally, in analyzing the pseudo-first-order reaction, Esfandian et al. noticed that adsorption processes in aqueous solutions by adsorbents followed the pseudo-first-order equation when the concentration of the adsorbed material in the aqueous solution was high, and at low concentrations of the adsorbed material the adsorption process matched the pseudo-second-order equation well [41].

8. Comparison of the Adsorbent with Other Adsorbents

Table 5 compares the maximum adsorption capacity of this adsorbent with those of others. Adsorption capacity of this adsorbent for copper was not high, and was only higher than the adsorption capacity of iron oxide nanoparticles coated on sand for copper. Therefore, this adsorbent is not recommended for copper removal from wastewater of the wood and paper factory.

CONCLUSIONS

SEM and FTIR were used to identify PPy/Perlite structure. Results suggested that the coating operation and polymer formation were carried out well. The optimum pH for adsorption of copper from the wastewater was 6. Moreover, the optimum contact time was 12 minutes and the optimum adsorbent dose 0.4 g/100 mL of the wastewater. Equilibrium data for both adsorption processes matched well with the Freundlich isotherm. The Kinetic data of adsorption matched well with the pseudo-second-order kinetic equation. Study of the effect of temperature on the adsorption process and study of the thermodynamics of the process showed that the adsorption process was spontaneous and endothermic.

REFERENCES

1. J. Kurczewska, G. Schroeder and U. Narkiewicz, *Open Chem.*, **8**, 341 (2010).
2. D. Pokhrel and T. Viraraghavan, *Sci. Total Environ.*, **333**, 37 (2004).
3. M. Jalilzadeh and S. Şenel, *J. Water Process. Eng.*, **13**, 143 (2016).
4. F. Ouadjenia-Marouf, R. Marouf, J. Schott and A. Yahiaoui, *Arab. J. Chem.*, **6**, 401 (2013).
5. H.-X. Zhu, X.-J. Cao, Y.-C. He, Q.-P. Kong and H. He, J. Wang, *Carbohydr. Polym.*, **129**, 115 (2015).
6. J. Acharya, J. Sahu, B. Sahoo, C. Mohanty and B. Meikap, *Chem. Eng. J.*, **150**, 25 (2009).
7. E. Derakhshani and A. Naghizadeh, *Desalin. Water Treat*, **52**, 7468 (2014).
8. Q.-Q. Zhong, Q.-Y. Yue, Q. Li, B.-Y. Gao and X. Xu, *Carbohydr. Polym.*, **111**, 788 (2014).
9. A. Naghizadeh and R. Nabizadeh, *Environ. Prot. Eng.*, **42**, 149 (2016).
10. A. R. Dinçer, Y. Güneş and N. Karakaya, *J. Hazard. Mater.*, **141**, 529 (2007).
11. N. Azbar, T. Yonar and K. Kestioglu, *Chemosphere*, **55**, 35 (2004).
12. O. E. A. Salam, N. A. Reiad and M. M. ElShafei, *J. Adv. Res.*, **2**, 297 (2011).
13. H. A. Hegazi, *HBRC J.*, **9**, 276 (2013).
14. K. G. bhattacharyya and S. S. Gupta, *Desalination*, **272**, 66 (2011).
15. F. Ji, C. Li, B. Tang, J. Xu, G. Lu and P. Liu, *Chem. Eng. J.*, **209**, 325 (2012).
16. S. Machida, S. Miyata and A. Techagumpuch, *Synth. Met.*, **31**, 311 (1989).
17. S. Rapi, V. Bocchi and G. P. Gardini, *Synth. Met.*, **24**, 217 (1988).
18. A. Tajik and R. M. A. Tehrani, *J. Appl. Chem.*, **10**, 159 (2015).
19. Z. B. Ouznadji, M. N. Sahmoune and N. Y. Mezenner, *Desalin. Water Treat*, **57**, 1880 (2016).
20. S. N. Azizi and N. Asemi, *J. Environ. Sci. Health Part B*, **47**, 692 (2012).
21. M. Omraei, H. Esfandian, R. Katal and M. Ghorbani, *Desalination*, **271**, 248 (2011).
22. R. Katal and H. Pahlavanzadeh, *J. Vinyl Addit. Technol.*, **17**, 138 (2011).
23. A. Naghizadeh, *Arab. J. Sci. Eng.*, **41**, 155 (2016).
24. H. Zavvar Mousavi and Z. Lotfi, *J. Appl. Chem.*, **7**, 49 (2012).
25. A. Naghizadeh, *J. Water Supply Res. Technol.-Aqua*, **64**, 64 (2015).
26. A.-J. A. Street, *World Appl. Sci. J.*, **13**, 331 (2011).
27. A. S. Bashammakh, *J. Mol. Liq.*, **220**, 426 (2016).
28. A. K. Bhattacharya, T. K. Naiya, S. N. Mandal and S. K. Das, *Chem. Eng. J.*, **137**, 529 (2008).
29. B. Kannamba, K. L. Reddy and B. V. AppaRao, *J. Hazard. Mater.*, **175**, 939 (2010).
30. A. Naghizadeh, H. Shahabi, F. Ghasemi and A. Zarei, *J. Water Health*, **14**, 989 (2016).
31. M. H. Dehghani, M. M. Taher, A. K. Bajpai, B. Heibati, I. Tyagi, M.

Asif, S. Agarwal and V. K. Gupta, *Chem. Eng. J.*, **279**, 344 (2015).
32. B. Singha and S. K. Das, *Colloids Surf. B-Biointerfaces*, **107**, 97 (2013).
33. B. Amarasinghe and R. Williams, *Chem. Eng. J.*, **132**, 299 (2007).
34. Y.-M. Hao, C. Man and Z.-B. Hu, *J. Hazard. Mater.*, **184**, 392 (2010).
35. Y.-C. Chang and D.-H. Chen, *J. Colloid Interface Sci.*, **283**, 446 (2005).
36. Y. Kuang, J. Du, R. Zhou, Z. Chen, M. Megharaj and R. Naidu, *J. Colloid Interface Sci.*, **447**, 85 (2015).
37. H. Chen, Y. Zhao and A. Wang, *J. Hazard. Mater.*, **149**, 346 (2007).
38. S. S. Madaeni and E. Salehi, *Chem. Eng. J.*, **150**, 114 (2009).
39. M. Malakootian, S. Mohammadi, N. Amirmahani, Z. Nasiri and A. Nasiri, *J. Community. Health Res.*, **5**, 89 (2016).
40. B. Ramavandi, M. Shamsi and N. Abdolahi, *Pajouhan Sci. J.*, **12**, 58 (2014).
41. H. Esfandian, M. Parvini, B. Khoshandam and A. Samadi-Maybodi, *Desalin. Water Treat*, **57**, 17206 (2016).
42. J. Lin, Y. Zhan and Z. Zhu, *Colloids Surf. A-Physicochem. Eng.*, **384**, 9 (2011).
43. W. W. Ngah, L. Teong, R. Toh and M. Hanafiah, *Chem. Eng. J.*, **209**, 46 (2012).
44. B. Al-Rashdi, C. Tizaoui and N. Hilal, *Chem. Eng. J.*, **183**, 294 (2012).
45. S.-M. Lee, C. Laldawngliana and D. Tiwari, *Chem. Eng. J.*, **195**, 103 (2012).